

## IMPORTANCE OF REFLECTED SOLAR ENERGY LOADED WITH SWCNTs-MWCNTs/EG DARCY POROUS STRETCHED SURFACE: MIDRICH SCHEME

 **Gunisetty Ramasekhar<sup>a\*</sup>**,  **Sangapatnam Suneetha<sup>b#</sup>**,  **Vanipenta Ravikumar<sup>c</sup>**,  **Shaik Jakeer<sup>d</sup>**,  
 **Seethi Reddy Reddissekhar Reddy<sup>c</sup>**

<sup>a</sup> Department of Mathematics, Rajeev Gandhi Memorial College of Engineering and Technology (Autonomous), Nandyal, 518501, Andhra Pradesh, India

<sup>b</sup> Department of Applied Mathematics Yogi Vemana University Kadapa, 516003, Andhra Pradesh, India

<sup>c</sup> Department of Mathematics, Annamacharya Institute of Technology and Sciences, (Autonomous), Rajampet, 516126, Andhra Pradesh, India

<sup>d</sup> School of Technology, The Apollo University, Chittoor, Andhra Pradesh, 517127, India

<sup>e</sup> Department of Mathematics, Koneru Lakshmaiah Education Foundation, Bowrampet, Hyderabad, Telangana, 500043, India

\*Corresponding Authors e-mail: [gunisettyrama@gmail.com](mailto:gunisettyrama@gmail.com), #e-mail [suneethayvu@gmail.com](mailto:suneethayvu@gmail.com)

Received November 29, 2023; revised December 18, 2023; accepted December 30, 2023

Saving energy, shortening processing times, maximizing thermal efficiency, and lengthening the life of industrial equipment are all possible outcomes of heating and cooling optimization. In recent years, there has been a rise in interest regarding the development of high-efficiency thermal systems for the purpose of enhancing heat and mass movement. This study presents an investigation on the non-linear flow of a hybrid nanofluid comprising of Multi Walled Carbon Nanotubes (MWCNTs) and Single Walled Carbon Nanotubes (SWCNTs) over an extended surface, considering the effects of Magnetohydrodynamics (MHD) and porosity, with engine oil serving as the base fluid. Also, radiation and Darcy-Forchheimer flow is considered. The problem of regulating flow is transformed into ordinary differential equations (ODEs) by employing similarity variables. The Midrich Scheme is then used to implement a numerical solution to these equations in the program Maple. Through visual representations of fluid velocities and temperatures, the inquiry addresses several important factors, including magnetic parameters, porosity parameters, radiation parameters, Eckert numbers, inertia coefficients, and Biot numbers. The research has important implications in a number of real-world contexts. Due to its exceptional characteristics, such as reduced erosion, reduced compression drops difficulties, and greatly increased heat transfer rates, hybrid nanofluids are frequently used in heat exchangers. For instance, various cooling devices such as electromagnetic cooling systems, as well as heat exchangers including condensers, boilers, chillers, air conditioners, evaporators, coil preheaters, and radiators. Furthermore, it has the potential to be employed in pharmaceutical businesses and the field of biomedical nanoscience.

**Keywords:** BVP Midrich scheme; MHD; Thermal radiation; Porous medium, Heat source; Darcy-Forchheimer flow; Hybrid nanofluid

**PACS:** 44.05.+e, 44.30.+v, 44.40.+a, 47.10.ad.

### INTRODUCTION

Because of its importance in a wide variety of engineering challenges and businesses, the issue of heat transfer continues to be one of the most hotly contested topics among scholars in the modern day. Nevertheless, water, oil, and glycol are commonly utilized in most applications, despite their poor thermal conductivity and inefficiency in facilitating heat transmission. To address this issue and enhance thermal efficiency, innovative fluid mediums, namely nano fluids and nanoparticles, are being created. Choi [1] was the first person to ever add metallic nanoparticles into base fluid for the purpose of increasing thermal conductivities and hence enhancing heat transfer. A few examples of real-world applications where nanofluids are employed to achieve higher levels of efficiency include the refrigerator, air conditioners, and other microelectronic goods as well as microcomputer processors. Researchers from all over the modern globe have been reporting their findings on the study of nano fluid, which has included both numerical and experimental research. Despite the significant advancements made in the field of nanofluids, contemporary researchers remain highly motivated and eager to explore novel fluid alternatives that surpass the thermal conductivity of nanofluids. Hybrid nanofluids, an advanced variation of nanofluids, have been developed to enhance performance and can serve as a suitable alternative to conventional nanofluids. Hybrid nanofluids consist of a combination of two modified types of nanoparticles. Compared to the base fluid and nanofluids made from a single type of nanoparticles, the hybrid nanofluid is predicted to have more advantageous thermal properties for heat transfer. Because of its superior performance, it is often referred to as a "next-generation fluid." Recently developed hybrid nanofluids have found widespread application in several fields of heat transmission. Microelectronics, microfluidics, transportation, manufacturing, medicine, military, acoustics, naval architecture, propulsion, and many more disciplines all fall under this broad category. The primary objective of utilizing hybrid nanofluids lies in the ability to strategically select an appropriate amalgamation of nanoparticles. This selection allows for the manipulation of the nanofluid, so augmenting the advantageous characteristics

associated with each particle type. Additionally, this approach serves to mitigate the drawbacks that arise from employing these particles individually, owing to the synergistic impact that arises from their combined utilization. The enhancement of thermal conductivity properties in hybrid nanofluids has garnered significant attention from researchers, leading to a substantial body of work focused on the practical applications of thermal transmission problems involving hybrid nanofluids. The investigation of heat transfer rate using hybrid nanofluid has emerged as a prominent field of study in recent years [2–6].

The thermo-physical and volume partitioning techniques are employed to ascertain the heat transport characteristics of nanomaterials. Nano fluids encompass a wide range of materials, including carbides, oxides, nitrides, fullerene, metals, and carbon nanotubes (CNTs), which are classified based on their size, form, and distinctive properties. The investigation of carbon nanotubes (CNTs) has been undertaken due to their heightened thermal conductivity properties. Carbon nanotubes, also known as CNTs, have a nanostructure resembling a barrel and are made up of numerous different allotropes of carbon. In the domains of health sciences, applied sciences, material sciences, energy, optics, natural sciences, and manufacturing, the morphological properties of carbon particles in spherical and tubular shapes are both intriguing and valuable. Single-walled carbon nanotubes (SWCNTs) and multi-walled carbon nanotubes (MWCNTs), which are differentiated from one another based on their structural properties, are the two unique categories that carbon nanotubes (CNTs) can be placed into. In 1991, Iijima [7] conducted a pioneering study on the application of CNTs in the examination of MWCNTs utilizing the Kratschmer and Huffman approach. The credit for the identification of SWCNTs is ascribed to Ajayan and Lijima in the year 1993 [8]. Over the past two decades, a substantial number of scholars have contributed a significant body of literature on the utilization of carbon nanotubes. The following selection of articles, ranging from references [9-16], may prove valuable for academic study purposes.

The field of fluid dynamics known as magnetohydrodynamic flow examines the magnetic properties of fluids that carry electricity and is a subfield of electrohydrodynamic flow. The application of magnetic fields in boundary layer flows serves the objective of causing separation of the boundary layer. A large number of researchers have included the impact of an external magnetic field effect into challenges involving hybrid nanofluid boundary layers. Magnetohydrodynamics, or MHD for short, offers a wide range of applications across a variety of business sectors and engineering subfields. Prominent applications of magnetohydrodynamic (MHD) technological innovations include controlled thermonuclear nuclear power plants, machines for refreshing shiny plates, power plants, circulatory control during surgical operations, magnetic endoscopy, magnetic devices utilized for cell separation, radiation therapy for cancer malignancy treatment, and magnetic targeting of medications. Magnetic endoscopy, magnetic cell separators, magnetic radiation therapy for tumors, and magnetic medication targeting are among further uses. In light of the aforementioned uses of the MHD, a significant number of researchers have investigated the MHD in the context of a variety of issues pertaining to fluid mechanics [17–19].

This study aim to examine the transport of hybrid nanofluid containing MWCNTs and SWCNTs over a stretched surface in presence of MHD and porosity with engine oil as base fluid. Also, radiation and Darcy-Forchheimer flow are taken into account. Notwithstanding the utility of the investigation, the flow model in question has not been formerly disseminated, and its flow features have not been subject to prior examination. The inquiry was prompted by the presence of multiple studies discussing the applications in industry and advancements of hybrid nanofluids. The mathematical model is solved by a computational approach known as the BVP Midrich method. The control problem can be effectively solved using Maple software, enabling the presentation of results through the use of figures and tables. This paper presents a qualitative analysis of the flow dynamics.

## MATHEMATICAL MODELING

In addition to a stretched surface, a two-dimensional heat transfer representation is examined in a mixed-heat-dispersal (MHD) SWCNTs and MWCNTs hybrid nanofluid. Within the framework of the energy and temperature equation, thermal radiation is taken into account. As can be seen in Table 1, two distinct kinds of nanoparticles, namely SWCNTs and MWCNTs, are suspended in the base fluid Engine oil. The velocity components  $u$  and  $v$  are measured along the  $x$ -axis and the  $y$ -axis, respectively; the velocity is written as  $u_w = ax$ . Furthermore, the temperature of the sheet as well as the temperature of the free stream is represented by the symbols  $T_w$ ,  $T_\infty$ , respectively, which is demonstrated in Figure 1.

**Table 1.** Thermophysical properties of Engine oil, SWCNTs-MWCNTs hybrid nanofluid [22]

Property	Engine oil	SWCNTs	MWCNTs
Density $\rho$ ( $kgm^{-3}$ )	884.00	2600.00	1600.00
Specific heat $C_p$ ( $Jkg^{-1}K^{-1}$ )	1910.00	425.00	796.00
Heat conductivity $k_f$ ( $Wm^{-1}K^{-1}$ )	0.1440	6600.00	3000.0
Electrical conductivity $\sigma$ ( $\Omega m$ ) <sup>-1</sup>	$10^{-6} - 2 \times 10^{-9}$	$10^{-16} - 10^8$	$10^6 - 10^7$
Pr	6450		

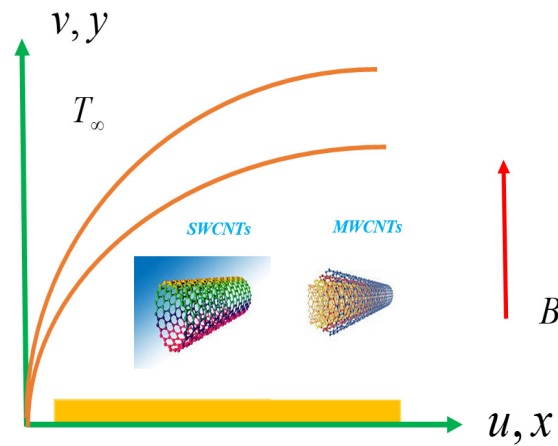


Figure. 1. Geometry of the problem

The governing flow equations are constructed as [20][21]

$$\frac{\partial u}{\partial x} + \frac{\partial v}{\partial y} = 0, \tag{1}$$

$$u \frac{\partial u}{\partial x} + v \frac{\partial u}{\partial y} = \frac{\mu_{hnf}}{\rho_{hnf}} \left( \frac{\partial^2 u}{\partial y^2} \right) - \frac{\mu_{hnf}}{\rho_{hnf}} \frac{u}{K^*} - F^* u^2 - \frac{\sigma_{hnf}}{\rho_{hnf}} (B^2 u), \tag{2}$$

$$u \frac{\partial T}{\partial x} + v \frac{\partial T}{\partial y} = \frac{k_{hnf}}{(\rho c_p)_{hnf}} \left( \frac{\partial^2 T}{\partial y^2} \right) - \frac{1}{(\rho c_p)_{hnf}} \left( \frac{\partial q_r}{\partial y} \right) + \frac{Q_0}{(\rho c_p)_{hnf}} (T - T_\infty) + \frac{\sigma_{hnf} B^2}{(\rho c_p)_{hnf}} u^2. \tag{3}$$

By Rosseland approach, we have

$$q_r = -\frac{4\sigma^*}{3k^*} \frac{\partial T^4}{\partial y}. \tag{4}$$

By applying the Taylor's series expansion of  $T^4$  about  $T_\infty$  and neglecting terms having higher order, we obtain

$$T^4 = 4T_\infty^3 T - 3T_\infty^4. \tag{5}$$

Putting Eq. (5) in Eq. (3), we get

$$u \frac{\partial T}{\partial x} + v \frac{\partial T}{\partial y} = \frac{k_{hnf}}{(\rho c_p)_{hnf}} \left( \frac{\partial^2 T}{\partial y^2} \right) - \frac{1}{(\rho c_p)_{hnf}} \frac{16T_\infty^3}{3k^*} \frac{\partial^2 T}{\partial y^2} + \frac{Q_0}{(\rho c_p)_{hnf}} (T - T_\infty) + \frac{\sigma_{hnf} B^2}{(\rho c_p)_{hnf}} u^2. \tag{6}$$

The corresponding boundary conditions are:

$$\begin{aligned} u = u_w(x) = ax, v = 0, k_{hnf} \frac{\partial T}{\partial y} = h_f (T_f - T), & \quad \text{at } y = 0 \\ u \rightarrow 0, T \rightarrow T_\infty & \quad \text{as } y \rightarrow \infty. \end{aligned} \tag{7}$$

The following suitable self-similarity transformations are defined as:

$$u = axf'(\eta), v = -\sqrt{av_f} f(\eta), \theta(\eta) = \frac{T - T_\infty}{T_f - T_\infty}, \eta = y \sqrt{\frac{a}{v_f}}. \tag{8}$$

Thermophysical properties of  $hnf$  are

$$R_1 = \frac{\mu_{hnf}}{\mu_f}, R_2 = \frac{\rho_{hnf}}{\rho_f}, R_3 = \frac{(\rho c_p)_{hnf}}{(\rho c_p)_f}, R_4 = \frac{k_{hnf}}{k_f}, R_5 = \frac{\sigma_{hnf}}{\sigma_f}.$$

$$\begin{aligned}
 R_1 &= \frac{1}{(1-\phi_1)^{2.5}(1-\phi_2)^{2.5}}, \\
 R_2 &= \left\{ (1-\phi_2) \left[ (1-\phi_1) + \phi_1 \left( \frac{\rho_{s_1}}{\rho_f} \right) \right] + \phi_2 \frac{\rho_{s_2}}{\rho_f} \right\}, \\
 R_3 &= (1-\phi_2) \left[ (1-\phi_1) + \phi_1 \left( \frac{(\rho c_p)_{s_1}}{(\rho c_p)_f} \right) \right] + \phi_2 \frac{(\rho c_p)_{s_2}}{(\rho c_p)_f}, \\
 R_4 &= \frac{k_{s_1} + 2k_{bf} - 2\phi_2(k_{bf} - k_{s_2})}{k_{s_2} + 2k_{bf} + \phi_2(k_{bf} - k_{s_2})} \times \frac{k_{s_1} + 2k_f - 2\phi_1(k_f - k_{s_1})}{k_{s_1} + 2k_f + \phi_1(k_f - k_{s_1})}, \\
 R_5 &= \frac{\sigma_{s_2} + 2\sigma_{nf} - 2\phi_2(\sigma_{nf} - \sigma_{s_2})}{\sigma_{s_2} + 2\sigma_{nf} + \phi_2(\sigma_{nf} - \sigma_{s_2})} \times \frac{\sigma_{s_1} + 2\sigma_f - 2\phi_1(\sigma_f - \sigma_{s_1})}{\sigma_{s_1} + 2\sigma_f + \phi_1(\sigma_f - \sigma_{s_1})}.
 \end{aligned} \tag{9}$$

In order to create the following dimensionless ODEs, Eqs. (2) and (6) are transformed using the ideal technique indicated in Eq (8).

$$\frac{R_1}{R_2} f''' + R_2 (ff'' - (f')^2) - \frac{R_1}{R_2} Kf' - Frf'^2 - \frac{R_5}{R_2} Mf' = 0, \tag{10}$$

$$\theta'' \left( R_4 + \frac{4}{3} Rd \right) + R_3 Prf\theta' + \frac{PrQ}{A_4} \theta + \frac{R_5}{R_3} MEc (f')^2 = 0. \tag{11}$$

The boundaries of the change are described as:

$$\begin{aligned}
 f(0) &= 0, f'(0) = 1, R_4\theta'(0) = -Bi(1 - \theta(0)) \\
 f'(\infty) &= 0, \theta'(\infty) = 0.
 \end{aligned} \tag{12}$$

Note that  $M = \frac{\sigma_f B^2}{\rho_f a}$  is the Magnetic field parameter,  $Pr = \frac{\mu_f (c_p)_f}{k_f}$  is the Prandtl number,  $Rd = \frac{4\sigma^* T_\infty^3}{k^* k_f}$  is the

Radiation parameter,  $Bi = \frac{h_f}{k_f} \sqrt{\frac{v_f}{a}}$  is the Biot number,  $Ec = \frac{a^2 x^2}{c_p (T_f - T_\infty)}$  is the Eckert number, and  $K = \frac{v_f}{aK^*}$  is the

porosity parameter,  $F^* = \left( \frac{C_d}{rK^{*1/2}} \right)$  non-uniform inertia coefficient, and  $Fr = \frac{C_d}{\sqrt{K^*}}$  inertia coefficient,  $Q = \frac{Q_0}{\Omega(\rho c_p)_f}$

heat absorption/generation coefficient.

The dimensional form of  $C_f$ , and  $Nu$  are expressed as

$$C_f = \frac{\tau_w}{\rho_f u_w^2} \tag{13}$$

Where shear stress  $\tau_w$  is  $\tau_w = \mu_{mf} \frac{\partial u}{\partial y} \Big|_{y=0}$

$$Nu = \frac{xq_w}{k_f (T_w - T_\infty)} \tag{14}$$

Where heat flux  $q_w$  is  $q_w = -k_{mf} \frac{\partial T}{\partial y} \Big|_{y=0}$

The non-dimensional form of Eqs. (13–14) converts are

$$Re_r^{1/2} C_f = CF = R_1 f''(0), \tag{15}$$

$$Re_r^{-1/2} Nu_r = Nu = -R_4 \theta'(0). \tag{16}$$

Where  $Re_r$  is the local Reynolds number.

**SOLUTION METHODOLOGY**

The nature of the ODE system (10–11) with BCs (12) is extremely nonlinear in its characteristics. For the purpose of dealing with these equations, we adopt a computational approach known as the BVP Midrich method see in Figure 2. Using Maple, we are able to solve the control problem. The midway method's standard operating procedure is laid out in detail below.

The following is a demonstration of the overall algorithm for the technique of midpoint collocation

$$\bar{Z}'(x) = F(x, \bar{Z}(x)), \quad \bar{Z}(x_0) = \bar{Z}_0, \tag{17}$$

In the explicit midpoint approach, also known as the Modified Euler method, the formula looks like this

$$\bar{Z}_{n+1} = \bar{Z}_n + hF\left(x_n + \frac{h}{2}, \bar{Z}_n + \frac{h}{2}F\left(x_n, \bar{Z}_n\right)\right), \tag{18}$$

The above equation  $h$  represents the step size and  $x_n = (x_0 + nh)$ .

The strategy that takes into account the implicit midpoint may be described as

$$\bar{Z}_{n+1} = \bar{Z}_n + hF\left(x_n + \frac{h}{2}, \bar{Z}_n + \frac{1}{2}(\bar{Z}_n, \bar{Z}_{n+1})\right), \quad n = 0, 1, 2, \dots \tag{19}$$

At each step size, the technique for locating the midpoint has a local error of order  $O(h^3)$  whereas the global error is of order  $O(h^2)$ . When dealing with algorithms that are more quantifiable demanding, the algorithm-error decreases at a quicker rate as  $h \rightarrow 0$  progresses, and the result gets more dependable.

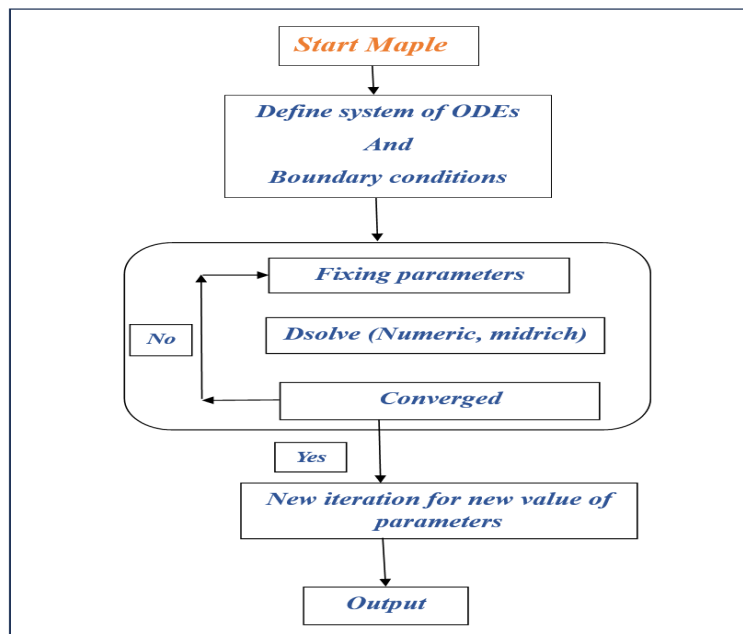


**Figure 2.** A flow chart pictogram of BVP Midrich technique

**RESULTS AND DISCUSSION**

The non-dimensional controlling flow model (10) – (11), which are subject to the boundary conditions (12), may be solved numerically with the assistance of Maple built in BVP Midrich scheme. We took the values of non-dimensional parameters and evaluated. Table 2, which illustrates the variances in skin friction coefficient, yields the exact solutions. The findings of both investigations were determined to be fairly accurate. Table 3, which demonstrates that various parameter values for CF. In the current part of the study, the authors go over the findings from the graphical narrative of the significant physical quantities in order to determine the quantitative fluctuation in relation to several important problem factors. To this end, writers have created graphs that define velocities, temperatures, Skin friction and heat transfer coefficient in order.

**Table 2.** Comparison table for various Prandtl numbers of the current study.

Pr	Ali et al. [20]	Present results
0.7	0.4560	0.4552902
2.0	0.9113	0.9101351

**Table 3.** The quantitative results of the skin friction coefficient of different of values for  $M$ ,  $Fr$  and  $K$  by fixing parameter values  $Rd = Bi = 0.4$ , and  $Pr = Ec = 0.1$ .

$M$	$Fr$	$K$	$CF$
0.1	0.4	0.5	1.026591
0.2	0.4	0.5	1.262674
0.3	0.4	0.5	1.004382
0.3	0.1	0.5	1.496002
0.3	0.2	0.5	1.172028
0.3	0.3	0.5	1.006005
0.3	0.4	0.1	0.958371
0.3	0.4	0.2	1.009034
0.3	0.4	0.3	1.045792

The influence of  $M$  on the velocity of MHD SWCNTs-MWCNTs/EG hybrid nanofluid is highlighted in Figure 3. Higher values of  $M$  cause some resistance in the fluid motion, as can be seen from the plot. The Lorentz forces, which are the resistive forces, increase in strength as  $M$  increases. when a result, when  $M$  increases, the Lorentz forces get stronger and slow down fluid motion.

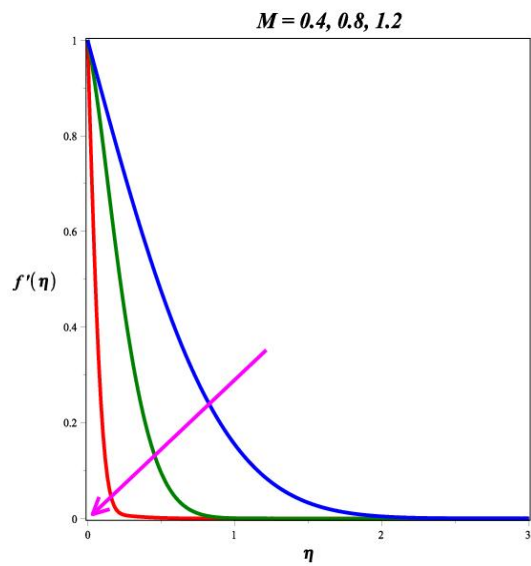


**Figure 3.** Pictogram of  $M$  on  $f'(\eta)$

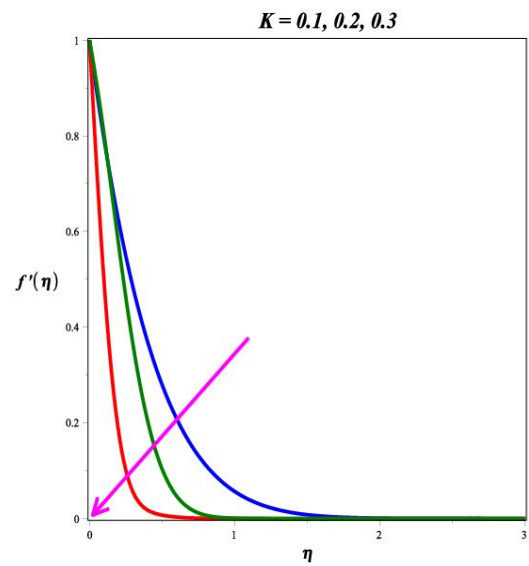


**Figure 4.** Pictogram of  $K$  on  $f'(\eta)$

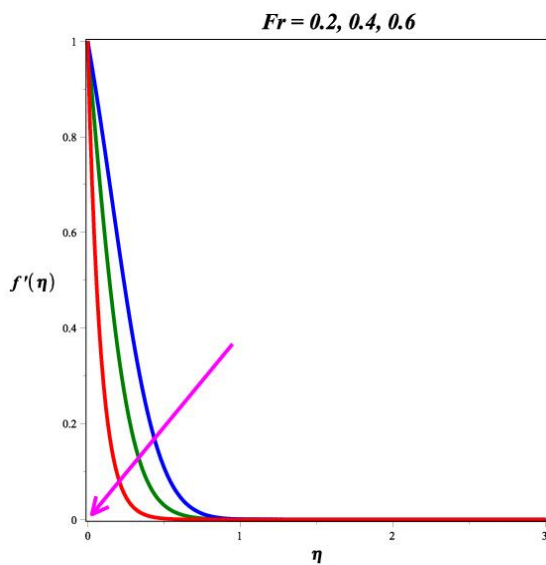


**Figure 5.** Pictogram of  $Fr$  on  $f'(\eta)$

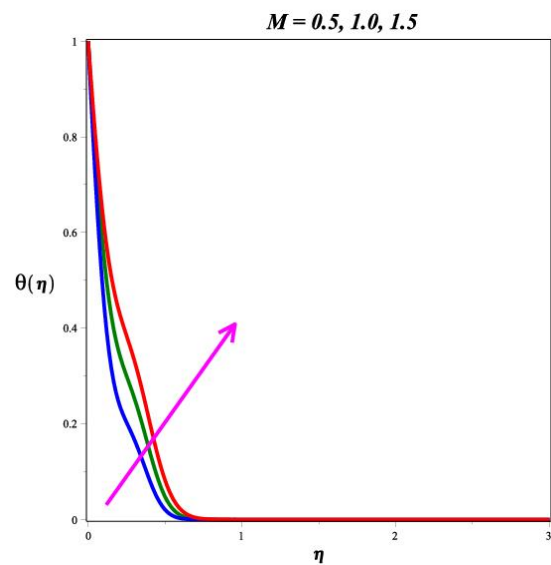


**Figure 6.** Pictogram of  $M$  on  $\theta(\eta)$

Figure 4 show the influence of the porous parameter  $K$  on the velocity of hybrid nanofluid. Raise in  $K$  essentially increases the difficulty of boundary layer separation. Additionally, as the frictional drag force increases, the boundary layer flow is not supported. Consequently, a downward tendency in the velocity pattern is observed for higher  $K$ .

Figure 5 describes the behavior of  $Fr$  on  $f'(\eta)$ . Large local inertia coefficient values, which lower fluid speed and boundary layer thickness, are indicative of enhanced medium porosity. Higher  $Fr$  causes the pores to enlarge, which ultimately lowers the speed.

The effect of the magnetic parameter ( $M$ ) on the temperature profile is depicted in Figure 6. Thermal energy strengthens the Lorentz force by motivating hybrid nanofluids to dissipate sub kinetic energy. In fact, as the magnetic factor increases, the size of the boundary layer's velocity profiles falls, leading to a raise in boundary layer temperature.

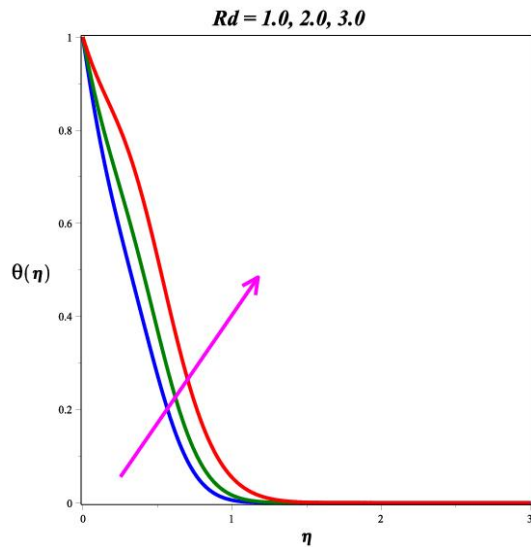


Figure 7. Pictogram of  $Rd$  on  $\theta(\eta)$

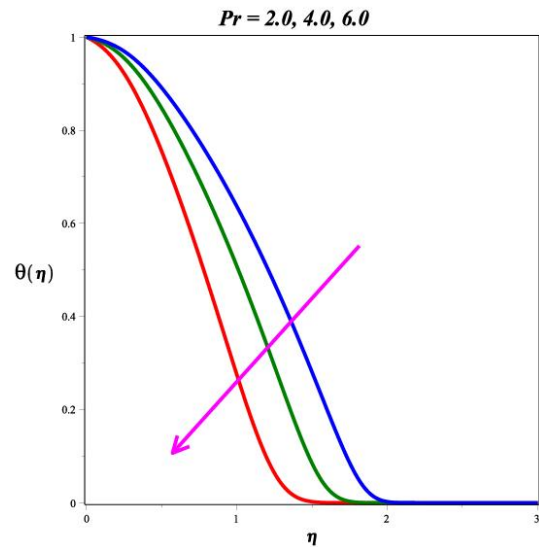


Figure 8. Pictogram of  $Pr$  on  $\theta(\eta)$

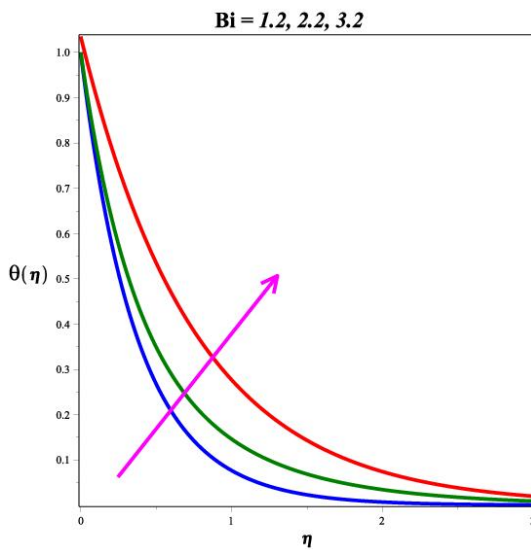


Figure 9. Pictogram of  $Bi$  on  $\theta(\eta)$

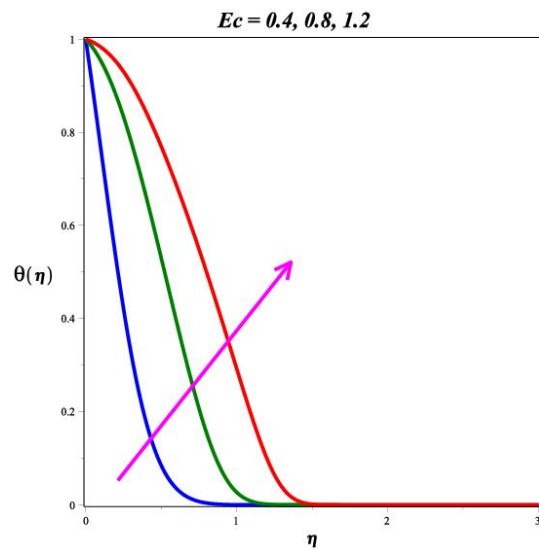


Figure 10. Pictogram of  $Ec$  on  $\theta(\eta)$

Figure 7 depicts the effect of various radiation parameter ( $Rd$ ) values on the temperature of hybrid nanofluid. Kinetic energy, or the energy required to cause moving atoms in matter to rotate, is derived from heated surfaces and is known as electromagnetic energy. The graph unequivocally demonstrates that better heat transmission results from raising the radiation parameter. A thicker thermal barrier layer is produced when the  $Rd$  parameter is raised because more heat is transported into the liquid. The temperature rises as the radiation parameter increases because the mean absorption coefficient drops. Thermal radiation has a positive physical effect on the medium's thermal diffusibility, which increases the temperature profile. Physically, higher temperature and a thicker thermal boundary layer are correlated with increased thermal radiation parameters.

The temperature for various amounts of  $Pr$  is revealed in Figure 8. It is clear that as  $Pr$  increases, the temperature parameter decreases. The boundary layer of thermal energy is thicker and the rate of heat transmission decreases for smaller  $Pr$ . Typically,  $Pr$  is employed in heat transfer-related applications to determine the width of the thermal and also the momentum border layers. This is due to the fact that when the Prandtl number increases, the thermal diffusion rate drops.

Figure 9 is aimed at presenting the variation in temperature with Biot number. The convective boundary property at the surface is connected to the Biot number. As the Biot number rises, the temperature gradient close to the surface also rises, raising the temperature there and, consequently, the thickness of the thermal boundary layer, as seen in Figure 9 the thermal resistance of a body as measured by its Biot number is the ratio of its internal thermal resistance to its surface thermal resistance.

Figure 10 describes the plot of temperature counter to the Eckert number  $Ec$ . The production of thermal energy increases with the existence of  $Ec$  in nanofluid, becoming more intense, improving temperature distributions, and therefore increasing thermal layer thickness. This is because frictional heating causes an increase in heat energy in the flow, which the viscosity of nanofluids stores and converts into internal energy when heated. From the same figure, it is noticed that the temperature is maximum near the walls when compared with the middle of the channel. Since  $Ec$  is proportional to the enthalpy of heat and to the kinetic energy of particles, an increase in  $Ec$  results in greater kinetic energy for the particles by decreasing the enthalpy actor, and thus an increase in temperature. Figure 11 depicts the inspiration of  $Q$  on energy outline. For the higher numeric values of the  $Q$  in energy profile enhanced. Physically, when heat generation rises, so does the inherent energy of liquid particles, resulting in a rise in the temperature outline.

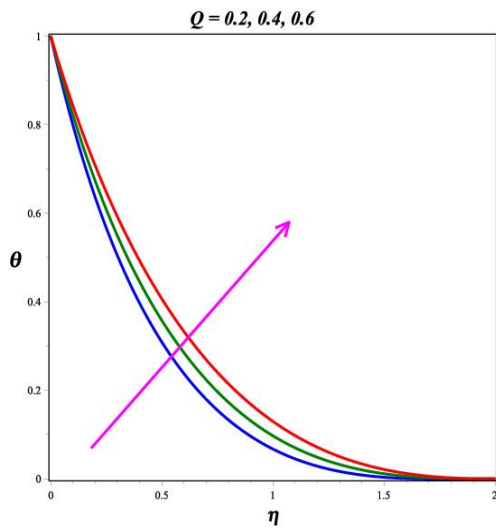


Figure 11. Pictogram of  $Q$  on  $\theta(\eta)$

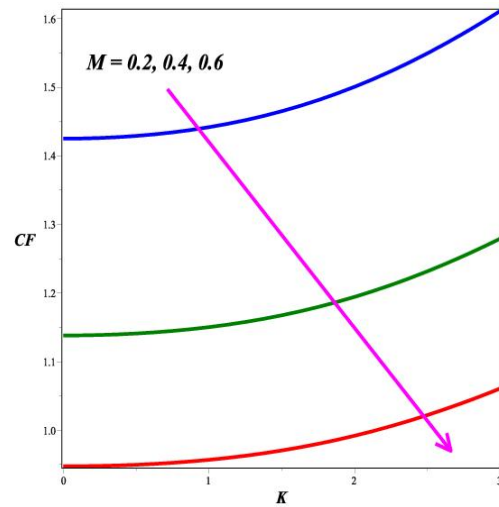


Figure 12. Sway of  $K$  and  $M$  on  $CF$

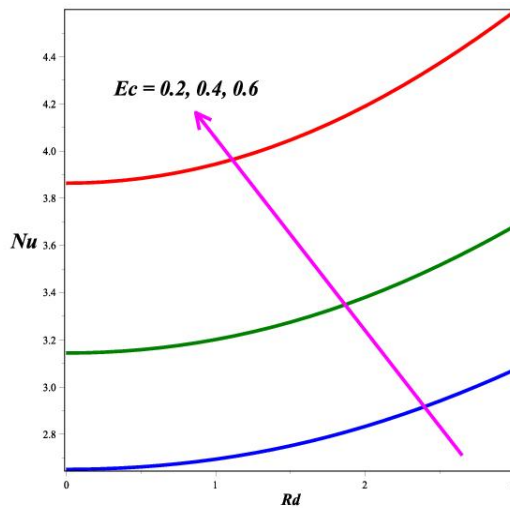


Figure 13. Sway of  $Rd$  and  $M$  on  $Nu$

The skin friction coefficient diminutions when growing the values of a magnetic parameter, similarly the skin friction increases when increasing porosity parameter is revealed in Figure 12. The effect of the radiation parameter and the Eckert number on the Nusselt number is shown in Figure 13. Increasing the Eckert number results in a corresponding rise in the Nusselt number and the radiation parameter. Plots or graphs of contours are frequently employed in the field of fluid dynamics for the purpose of visualizing and analyzing numerous characteristics included inside a liquid, including its speed, pressure, energy, and concentration. For the higher values of the magnetic parameter case, we are observing on decreasing tendency which is presented in Figures 14 and 15, while the opposite nature we noticed on Nusselt number profile and it is demonstrated in Figures 16 and 17.

The various values of  $M$ ,  $K$ ,  $Fr$  were presented in Figures 18, 19, and 20. Rising porosity liquid medium leads to reduced magnetic field for the movement of fluids, as seen in the graph. A decreased heat transfer rate is seen for moving sheet. Streamlines have significance in the study of fluids and technology for many different reasons. Streamlines illustrate movement of fluids characteristics. They demonstrate fluid particle movement and path throughout period. This simplifies unpredictable interpretation.

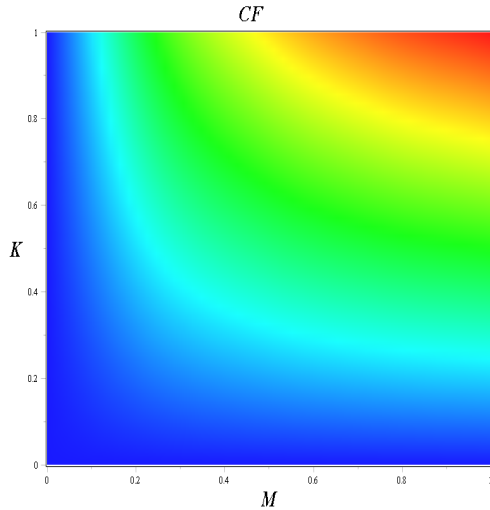


Figure 14. Sway of  $K$  and  $M$  on  $CF$

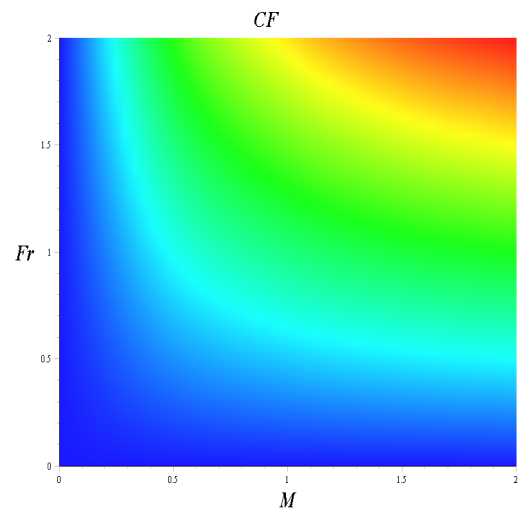


Figure 15. Sway of  $Fr$  and  $Rd$  on  $CF$

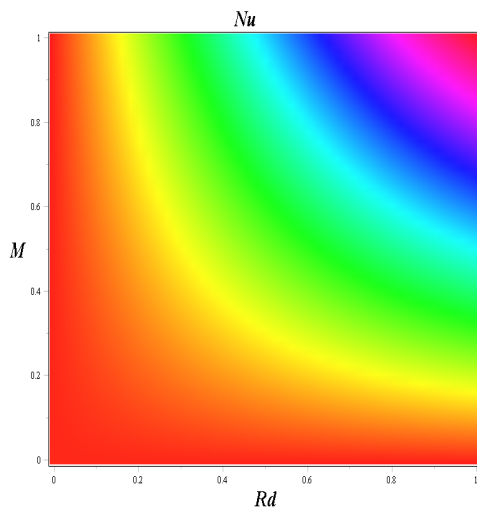


Figure 16. Sway of  $Fr$  and  $Rd$  on  $Nu$

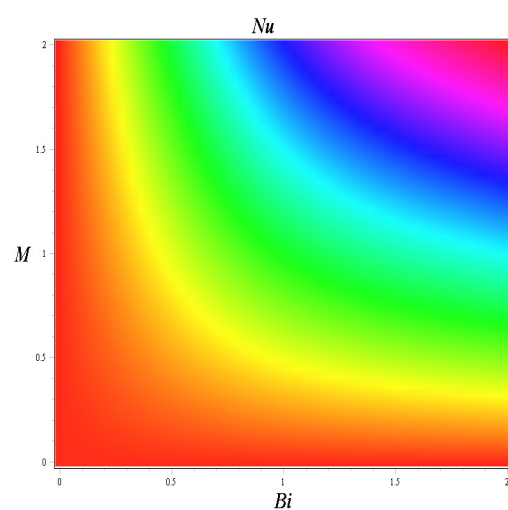


Figure 17. Sway of  $Fr$  and  $Rd$  on  $Nu$

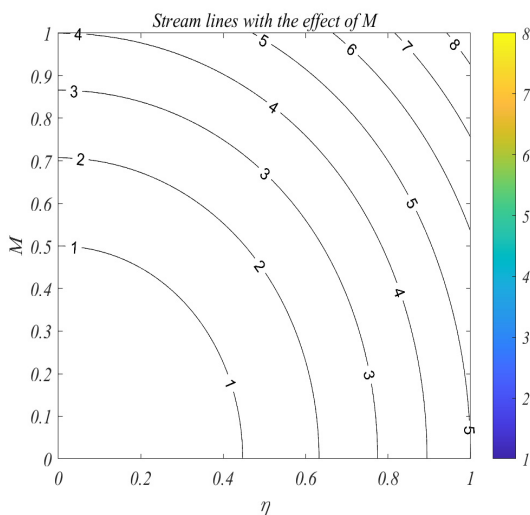


Figure 18. Stream lines for  $M$

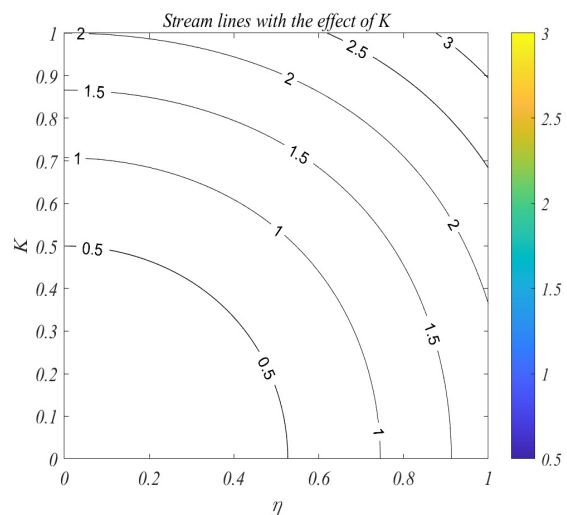


Figure 19. Stream lines for  $K$

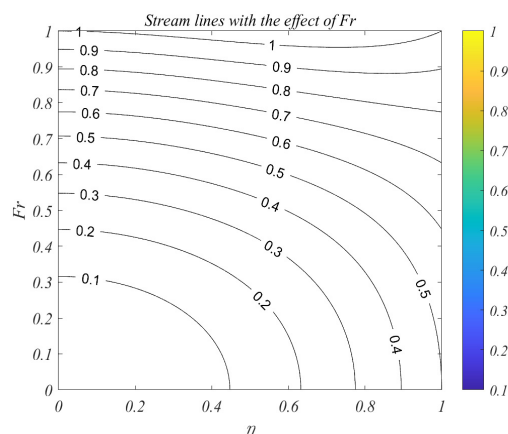


Figure 20. Stream lines for  $Fr$

### CONCLUSIONS

The current research study explored the numerical solution for MHD of SWCNTs-MWCNTs /Engine oil hybrid nanofluid over a Stretching surface. The Numerical method (BVP Midrich scheme) was used to solve the issue of velocity, temperature and the outcome was truly solution to the model. The results are presented in a variety of graphical formats, including a two-dimensional plot, Contour plots, and streamlines.

The research produced a number of interesting findings, which are listed below:

1. The high local inertia coefficient values, which lower both the fluid velocity and the boundary layer thickness.
2. Thermal radiation has a positive physical effect on the medium's thermal diffusibility, which increases the temperature profile of the hybrid nanofluid.
3. The temperature gradient at the surface rises with a rise in the Biot number, raising the temperature there and, consequently, the thickness of the thermal boundary layer.
4. When the value of  $Ec$  is increased, it results in an elevation in the kinetic energy of particles due to a decrease in the enthalpy factor. This increase in kinetic energy subsequently leads to a rise in temperature.
5. By enhancing the values of the Eckert number, increases the Nusselt number and the radiation parameter.
6. As the values of the radiation parameter and magnetic field parameter are increased, the rate of skin friction increases.
7. Magnetic parameter strength draws electrical conductivity molecules more towards to the main stream is observed on streamlines plots.

### ORCID

©Gunisetty Ramasekhar, <https://orcid.org/0000-0002-3256-3145>; ©Sangapatnam Suneetha, <https://orcid.org/0000-0001-6627-6446>

©Vanipenta Ravikumar, <https://orcid.org/0000-0001-9598-8717>; ©Shaik Jakeer, <https://orcid.org/0000-0002-6350-1457>

©Seethi Reddy Reddisekhar Reddy, <https://orcid.org/0000-0001-5501-570X>

### REFERENCES

- [1] S.U. Choi, and J.A. Eastman, *Enhancing Thermal Conductivity of Fluids with Nanoparticles*, Technical Report, (Argonne National Lab. Argonne, IL, USA, 1995).
- [2] A. Venkateswarlu, S. Suneetha, M.J. Babu, J.G. Kumar, C.S.K. Raju, and Q. Al-Mdallal, "Significance of Magnetic Field and Chemical Reaction on the Natural Convective Flow of Hybrid Nanofluid by a sphere with viscous dissipation: A statistical Approach," *Nonlinear Engineering*, **10**, 563–573 (2021). <https://doi.org/10.1515/nleng-2021-0047>
- [3] A.B. Vishalakshi, R. Mahesh, U.S. Mahabaleswar, A.K. Rao, L.M. Pérez, and D. Laroze, "MHD Hybrid Nanofluid Flow over a Stretching/Shrinking Sheet with Skin Friction: Effects of Radiation and Mass Transpiration," *Magnetochemistry*, **9**, 118 (2023). <https://doi.org/10.3390/magnetochemistry9050118>
- [4] P.S. Reddy, P. Sreedevi, and A.J. Chamkha, "Hybrid Nanofluid Heat and Mass Transfer Characteristics Over a Stretching/Shrinking Sheet with Slip Effects," *Journal of Nanofluids*, **12**, 251–260 (2023). <https://doi.org/10.1166/jon.2023.1996>
- [5] U. Farooq, M. Tahir, H. Waqas, T. Muhammad, A. Alshehri, and M. Imran, "Investigation of 3D flow of magnetized hybrid nanofluid with heat source/sink over a stretching sheet," *Sci. Rep.* **12**(1), 12254 (2022). <https://doi.org/10.1038/s41598-022-15658-w>
- [6] M. Nadeem, I. Siddique, J. Awrejcewicz, *et al.*, "Numerical analysis of a second-grade fuzzy hybrid nanofluid flow and heat transfer over a permeable stretching/shrinking sheet," *Sci. Rep.* **12**, 1631 (2022). <https://doi.org/10.1038/s41598-022-05393-7>
- [7] S. Iijima, "Helical microtubules of graphitic carbon," *Nature*, **354**, 56–58 (1991). <https://doi.org/10.1038/354056a0>
- [8] P.M. Ajayan, and S. Iijima, "Capillarity-induced filling of carbon nanotubes," *Nature*, **361**, 333–334 (1993). <https://doi.org/10.1038/361333a0>
- [9] K. Subbarayudu, S. Suneetha, P.B.A. Reddy, and A.M. Rashad, "Framing the activation energy and binary chemical reaction on CNT's with Cattaneo-Christov heat diffusion on Maxwell Nano fluid in the presence of non-linear thermal radiation," *Arabian journal of Science and Engineering*, **44**, 10313–10325 (2019). <https://doi.org/10.1007/s13369-019-04173-2>

- [10] L. Wahidunnisa, S. Suneetha, S.R.R. Reddy, and P.B.A. Reddy, "Comparative study on electromagnetohydrodynamic SWCNT-water dusty nanofluid in the presence of radiation and Ohmic heating," Proceedings of the Institution of Mechanical Engineers, Part E: Journal of Process Mechanical Engineering, **235**(4), 950-958 (2021). <https://doi.org/10.1177/0954408920985735>
- [11] S. Suneetha, L. Wahidunnisa, A. Divya, and P.B.A. Reddy, "Electrical magnetohydrodynamic flow of kerosene oil-based carbon nanotube's Maxwell nanofluid in the presence of non-linear radiation and Cattaneo-Christov heat diffusion: Applications in aerospace industry," Proc. Mech. E, Part E: J. Process Mechanical Engineering, **237**, 1670-1678 (2022). <https://doi.org/10.1177/09544089221125100>
- [12] G. Ramasekhar, and P.B. Reddy, "Numerical analysis of significance of multiple shape factors in Casson hybrid nanofluid flow over a rotating disk," International Journal of Modern Physics B, **37**(12), 2350113 (2023). <https://doi.org/10.1142/S0217979223501138>
- [13] R. Tabassum, A. Al-Zubaidi, S. Rana, R. Mehmood, and S. Saleem, "Slanting transport of hybrid (MWCNTs-SWCNTs/H<sub>2</sub>O) nanofluid upon a Riga plate with temperature dependent viscosity and thermal jump condition," International Communications in Heat and Mass Transfer, **135**, 106165 (2022). <https://doi.org/10.1016/j.icheatmasstransfer.2022.106165>
- [14] E. Tayari, L. Torkzadeh, D. Domiri Ganji, et al., "Investigation of hybrid nanofluid SWCNT-MWCNT with the collocation method based on radial basis functions," Eur. Phys. J. Plus, **138**, 3 (2023). <https://doi.org/10.1140/epjp/s13360-022-03601-x>
- [15] A.M. Obalalu, M.A. Memon, and O.A. Olayemi, et al., "Enhancing heat transfer in solar-powered ships: a study on hybrid nanofluids with carbon nanotubes and their application in parabolic trough solar collectors with electromagnetic controls," Sci. Rep. **13**, 9476 (2023). <https://doi.org/10.1038/s41598-023-36716-x>
- [16] Z. Shah, A. Tassaddiq, S. Islam, A.M. Alkhalibi, and I. Khan, "Cattaneo-Christov heat flux model for three-dimensional rotating flow of SWCNT and MWCNT nanofluid with Darcy-Forchheimer porous medium induced by a linearly stretchable surface," Symmetry, **11**(3), 331 (2019). <https://doi.org/10.3390/sym11030331>
- [17] G. Ramasekhar, and P.B.A. Reddy, "Entropy generation on Darcy-Forchheimer flow of copper-aluminium oxide/water hybrid nanofluid over a rotating disk: Semi-analytical and numerical approaches," Scientia Iranica. Transaction F, Nanotechnology, **30**(6), 2245-2259 (2023). <https://doi.org/10.24200/sci.2023.60134.6617>
- [18] I. Rashid, T. Zubair, and M.I. Asjad, "Tag-Eldin E.M. The Influence of Aligned MHD on Engine Oil-Based Casson Nanofluid with Carbon Nanotubes (Single and Multi-Wall) Passing through a Shrinking Sheet with Thermal Radiation and Wall Mass Exchange," Micromachines (Basel), **13**(9), 1501 (2022). <https://doi.org/10.3390/mi13091501>
- [19] S.R.R. Reddy, P.B.A. Reddy, and S. Suneetha, "Magnetohydro Dynamic Flow of Blood in A Permeable Inclined Stretching Viscous Dissipation, Non-Uniform Heat Source/Sink and Chemical Reaction," Frontiers in Heat and Mass Transfer, **10**(22), 1-10 (2018). <https://doi.org/10.5098/hmt.10.22>
- [20] M. Ramzan, F. Ali, N. Akkurt, et al., "Computational assesment of Carreau ternary hybrid nanofluid influenced by MHD flow for entropy generation," J. Magn. Magn. Mater. **567**, 170353 (2023). <https://doi.org/10.1016/j.jmmm.2023.170353>
- [21] G. Ramasekhar, and P.B.A. Reddy, "Entropy generation on EMHD Darcy-Forchheimer flow of Carreau hybrid nano fluid over a permeable rotating disk with radiation and heat generation: Homotopy perturbation solution," Proc. Inst. Mech. Eng. Part E, J. Process Mech. Eng. **237**(4), 1179-1191 (2022). <https://doi.org/10.1177/09544089221116575>
- [22] S. Ahmad, S. Nadeem, N. Muhammad, and A. Issakhov, "Radiative SWCNT and MWCNT nanofluid flow of Falkner-Skan problem with double stratification," Phys. A, Stat. Mech. Appl. **547**, 124054 (2020). <https://doi.org/10.1016/j.physa.2019.124054>

### ВАЖЛИВІСТЬ ВІДБИТОЇ СОНЯЧНОЇ ЕНЕРГІЇ, ДЛЯ НАВАНТАЖЕНОЇ SWCNTs-MWCNTs/EG, ПОРИСТОЇ РОЗТЯГНУТОЇ ПОВЕРХНІ DARCY: СХЕМА МІДРІХА

Рамасекхар Гунісетті<sup>a</sup>, Сангапатнам Сунітха<sup>b</sup>, Ваніпента Равікумар<sup>c</sup>, Шайк Джакер<sup>d</sup>, Сіті Редді Реддісекар Редді<sup>e</sup>

<sup>a</sup> Кафедра математики, Меморіальний коледж інженерії та технологій імені Раджива Ганді (автономний), Нандьял, 518501, Андхра-Прадеш, Індія

<sup>b</sup> Департамент прикладної математики Університет Йогі Вемана Кадапа, 516003, Андхра-Прадеш, Індія

<sup>c</sup> Департамент математики, інститут технологій і наук Аннамачарья, (автономний), Раджампет, 516126, Андхра-Прадеш, Індія

<sup>d</sup> Школа технологій, Університет Аполло, Читтор, Андхра-Прадеш, 517127, Індія

<sup>e</sup> Департамент математики, Освітня фундація Конеру Лакимайя, Боурампет, Хайдарабад, Телангана, 500043, Індія

Економія енергії, скорочення часу обробки, максимізація термічної ефективності та подовження терміну служби промислового обладнання – усі можливі результати оптимізації опалення та охолодження. Останніми роками зріс інтерес до розробки високоефективних теплових систем з метою підвищення тепло- та масопереміщення. У цьому дослідженні представлено дослідження нелінійного потоку гібридної нанофлюїду, що складається з багатостінних вуглецевих нанотрубок (MWCNT) і одностінних вуглецевих нанотрубок (SWCNT) над розтягнутою поверхнею, враховуючи вплив магнітогідродинаміки (МНД) і пористості, з масляним двигуном, яке служить базовою рідиною. Також враховується радіація та потік Дарсі-Форхгеймера. Задача регулювання потоку перетворюється на звичайні диференціальні рівняння за допомогою змінних подібності. Схема Мідріха потім використовується для реалізації чисельного розв'язку цих рівнянь у програмі Maple. За допомогою візуального представлення швидкостей і температур рідини запит стосується кількох важливих факторів, включаючи магнітні параметри, параметри пористості, параметри випромінювання, числа Еккерта, коефіцієнти інерції та числа Віот. Дослідження має важливі наслідки в багатьох контекстах реального світу. Завдяки своїм винятковим характеристикам, таким як зменшення ерозії, зменшення труднощів падіння при стисненні та значно підвищена швидкість теплопередачі, гібридні нанофлюїди часто використовуються в теплообмінниках. Наприклад, різні охолоджувальні пристрої, такі як електромагнітні системи охолодження, а також теплообмінники, включаючи конденсатори, котли, чиллери, кондиціонери, випарники, змійовики попереднього нагрівання та радіатори. Крім того, він має потенціал для використання у фармацевтичному бізнесі та в галузі біомедичної нанонауки.

**Ключові слова:** схема VVP Midrich; МГД; теплове випромінювання; пористе середовище, джерело тепла; потік Дарсі-Форхгеймера; гібридний нанофлюїд